Applied Catalysis A: General 497 (2015) 58–71

Contents lists available at ScienceDirect

Applied Catalysis A: General

journal homepage: www.elsevier.com/locate/apcata

# Ga and In promoters in bimetallic Pt based catalysts to improve the performance in the selective hydrogenation of citral

Julieta P. Stassi*, Patricia D. Zgolicz, Virginia I. Rodríguez, Sergio R. de Miguel, Osvaldo A. Scelza

*Instituto de Investigaciones en Catálisis y Petroquímica (INCAPE) "Ing. José Miguel Parera", Facultad de Ingeniería Química, Universidad Nacional del Litoral, CONICET, Santiago del Estero 2654, 3000 Santa Fe, Argentina*

ARTICLE INFO

*Article history:*
Received 13 November 2014
Received in revised form 28 January 2015
Accepted 31 January 2015
Available online 27 February 2015

*Keywords:*
Multiwall carbon nanotubes
Carbon Vulcan XC-72
Bimetallic catalysts
Metallic phase characterization
Citral hydrogenation

ABSTRACT

In this paper, bimetallic PtGa and PtIn catalysts supported on multiwall carbon nanotubes and carbon Vulcan were used to study the hydrogenation of citral (α,β-unsaturated aldehyde) in liquid phase to produce nerol and geraniol (unsaturated alcohols, UA). The catalysts were prepared with different metallic loadings by conventional impregnation. All the catalysts contained a Pt loading of 5 wt%. Once reduced under hydrogen flow, the supported catalysts were characterized by test reactions of the metallic phase, $H_2$ chemisorption, temperature programmed reduction (TPR), X-ray photoelectron spectroscopy (XPS) and transmission electron microscopy (TEM). Hydrogenation results showed that the addition of a second metal to Pt leads to important modifications of the selectivity to UA. The highest selectivities to UA were reached with different promoter/Pt atomic ratios for Ga and In. The catalyst performances in the citral hydrogenation were related to the characteristics of each supported bimetallic phase. It was found that the PtGa catalysts have a typical behavior of an ionic promoter together with a contribution of the Ga reduced species, reaching high selectivities to UA. On the other hand, PtIn catalysts with a metallic phase composed mainly by zerovalent In species in contact with the metallic phase, also showed high activities and selectivities to UA. The best selectivity value to UA (about 97%) was found for PtIn(2.5 wt%)/CN-P catalyst with an excellent activity.



## 1. Introduction

Citral is an α,β-unsaturated aldehyde which contains two double conjugated bonds (one carbonyl group and one double bond conjugated with that group), and an isolated double bond. These characteristics make citral an interesting model molecule to study selective hydrogenation reactions, from a scientific point of view to an industrial one [1]. This reaction is a very important one mainly for the preparation of different fine chemicals, for example menthol which is obtained via cyclization and has several uses in pharmaceutical industries [2]. Besides, fine chemicals such as unsaturated alcohols obtained from the citral hydrogenation are intermediary materials for the development of perfumes, flavors and pharmaceutical products [3].

Heterogeneous catalysts have several advantages with respect to homogeneous ones, such as easy separation, handling and recycling of the catalyst. An efficient strategy is to graduate the selectivity using a catalyst of specific characteristics [4]. In fine chemical industry, catalysts based on precious metals and supported on carbonaceous materials are frequently used, giving excellent performances in hydrogenation reactions [5]. However, bimetallic catalysts based on Pt with some p-block metals as promoters (In, Ga) were rarely studied.

Good selectivities to unsaturated alcohols in α,β-unsaturated aldehydes hydrogenation reactions were found using PtSn catalysts supported on different materials [6,7]. In this case the interaction of the ionic Sn species with the oxygen of the carbonyl group could weaken the C=O bond and enhance the carbonyl hydrogenation rate. Besides, it is possible that the presence of metal alloys or a strong metal–promoter interaction leads to an increase of the Pt electron density decreasing the adsorption of the C=C bond. This fact would favor the interaction with the carbonyl group [8,9].

It is known that microporous carbons are normally employed as supports of active metals for the preparation of catalysts to be used in selective hydrogenation reactions, but the use of mesoporous carbons (with lower specific surface area) has been scarcely explored in the literature. In fact few papers about the use of

* Corresponding author. Tel.: +54 342 4555279.
*E-mail address:* jstassi@fiq.unl.edu.ar (J.P. Stassi).

http://dx.doi.org/10.1016/j.apcata.2015.01.046
0926-860X/

**Table 1**
Surface area ($S_{BET}$), pore volume ($V_{pore}$) and isoelectric points (p*I*) of carbon Vulcan (CV) and carbon nanotubes after purification (CN-P) [9].

| Support | $S_{BET}$ ($m^2\,g^{-1}$) | $V_{pore}$ ($cm^3\,g^{-1}$) | p*I* |
|---|---|---|---|
| CV | 240 | 0.36 | 7.4 |
| CN-P | 179 | 0.39 | 4.7 |

carbon Vulcan and nanotubes as supports of metals in the selective hydrogenation of citral have been reported [10–13]. Thus, the scientific information about selective hydrogenation of α,β-unsaturated aldehydes using catalysts supported on carbon Vulcan is scarce. Moreover, there are not complete studies about bimetallic catalysts supported on carbon nanotubes. It is known that PtSn catalysts supported on these materials lead to a very high selectivity to unsaturated alcohols (UA: nerol + geraniol) with a very good activity [9]. Other p-block metals, such as Ga and In, are commonly used as promoters in other reactions such as dehydrogenation ones [14–17]. Besides, Ga addition to Pt leads to an important promotion effect in some selective hydrogenation reactions [18–20], but there are no studies of the PtIn couple for the selective hydrogenation of α,β-unsaturated aldehydes. The interaction between the active metal (Pt) and the promoters (Ga or In) is not well-known, so it is not possible to know how these two metals interact to give a favorable promoter effect. Therefore, the characterization and determination of the catalytic behavior of these catalysts would be of great interest. In this paper, PtGa and PtIn bimetallic catalysts supported on two types of carbonaceous materials (carbon Vulcan and multiwall carbon nanotubes) were studied by using different loading of the promoters and evaluated in selective hydrogenation of citral. This work seeks to achieve high production of unsaturated alcohols (geraniol and nerol) from citral hydrogenation, with excellent selectivities to UA.

## 2. Experimental

Two commercial carbonaceous supports were selected: (i) carbon black Vulcan XC-72 (granular carbon from Cabot Corp., purity >99%), which was called CV; (ii) multiwall carbon nanotubes (MWCN from Sunnano, purity >90%, diameter 10–30 nm, length 1–10 μm), which were called CN. Carbon Vulcan was used in its original form because its impurity levels were very low (0.45%). On the other hand, carbon nanotubes were purified in order to eliminate impurities (about 6%), such as metals and other compounds, that could be negative for the final catalyst. Purified carbon nanotubes were called CN-P. The impurity levels of the supports were determined by EDX and the experimental details of the purification process were given in a previous work [9].

Both supports were previously characterized in order to know their textural properties ($S_{BET}$ and $V_{pore}$) and their acid character (isoelectric point, p*I*). These results were reported in a previous work [9] and are shown in Table 1. It was found that the supports present quite similar textural properties, but their acid character, determined by titration, was different. In spite of this, both carbon nanotubes and carbon Vulcan show an amphoteric behavior and display a very good adsorption of the metals during the impregnation step [9,21].

All the bimetallic catalysts were prepared by successive impregnation of the corresponding monometallic ones. Thus, monometallic catalysts were prepared by conventional impregnation of the corresponding support with an aqueous solution of $H_2PtCl_6$ (Johnson Matthey Inc.) at 25 °C for 6 h. In all cases, the Pt amount used for the impregnation was the appropriate to obtain a Pt content of 5 wt%. In order to achieve uniform contact between the solid and the impregnating solution, a stirring rate of 250 rpm was used and the impregnating volume/support weight ratio was 30 mL $g^{-1}$. The excess of solution was evaporated at low temperature after impregnation until a paste was formed. Then, the samples were dried overnight at 120 °C and then they were crushed to a powder.

PtGa and PtIn bimetallic catalysts over both supports were prepared by the impregnation of the monometallic Pt one with the corresponding precursor ($Ga(NO_3)_3$, Sigma–Aldrich 99.9% and $In(NO_3)_3$, Alfa Aesar 99.9%) using the same conditions mentioned above for monometallic catalysts. Thus, each portion of monometallic catalyst was impregnated to obtain the corresponding loadings of the second metal (Ga: 0.6, 1.8, 3.12 wt% and In: 0.97, 1.94, 2.5, 2.95 wt%). Finally, all samples were dried overnight at 120 °C and then crushed to a powder. After conventional impregnation, all catalysts were reduced at 350 °C under hydrogen flow for 3 h. In the same way, the monometallic Ga and In catalysts were prepared by conventional impregnation of the supports with the corresponding precursors.

Additionally, some selected catalysts were submitted to further thermal treatment in order to induce sinterization and/or modification of the metallic phase [21]. The thermal treatment was applied after the reduction treatment mentioned before. It consisted on maintaining the selected samples under nitrogen flow at 700 °C for 12 h. These catalysts were referred in the text by the denomination of the corresponding catalysts followed by —$N_2$. Table 2 shows the sample compositions according to the preparation method of the catalysts.

Two test reactions were selected to study the metallic phase of catalytic samples: cyclohexane dehydrogenation (CHD) [22] and cyclopentane hydrogenolysis (CPH) [23,24]. They were performed in a differential continuous flow reactor at 250 and 350 °C, respectively. In both reactions the catalysts were previously reduced "in situ" under $H_2$ flow at 350 °C for 3 h. The experiments were performed by using $H_2$/CH and $H_2$/CP molar ratios equal to 26 and 29, respectively, and a volumetric flow of 600 mL $H_2$ $min^{-1}$ in both reactions. The catalyst weight used in these test reaction experiments was such as to obtain a conversion lower than 5%, since under these conditions the behavior of the reactor follows a differential flow reactor model that allows the correct measurement of the initial rate and activation energy. The reaction products and the remaining reactants were analyzed by using a gas chromatographic system. The activation energy values for CHD ($Ea_{CH}$) were calculated by linear regression using the reaction rates measured at three temperatures (250, 240 and 230 °C) and the Arrhenius plot ($\ln R^0_{CH}$ vs. $1/T\,(K^{-1})$).

The $H_2$ chemisorption measurements were carried out in a volumetric equipment. The sample weight used in the experiments was 200 mg. All the catalysts were previously reduced in $H_2$ at 350 °C for 3 h, then outgassed under high vacuum ($10^{-5}$ T). The $H_2$ adsorption isotherms were performed at room temperature between 25 and 100 T. The isotherms were linear in the range of used pressures and the $H_2$ chemisorption capacity was calculated by extrapolation of the isotherms to zero pressure [25].

Temperature programmed reduction (TPR) experiments were performed using a reductive mixture of $H_2$ (5%, v/v)–$N_2$ with a flow rate of 9 mL $min^{-1}$ in a flow reactor and a sample weight of 200 mg. Samples were heated at 6 °C $min^{-1}$ from 25 up to 800 °C. The exit of the flow reactor was connected to a TCD (thermal conductivity detector) in order to obtain the TPR signal. Before TPR experiments, the dried samples were stabilized with $N_2$ at room temperature for 1 h.

XPS determinations were carried out in a Multitechnic Specs photoemission electron spectrometer equipped with an X-ray source Mg/Al and a hemispherical analyzer PHOIBOS 150 in the fixed analyzer transmission mode (FAT). The spectrometer operates with an energy power of 100 eV and the spectra were obtained with

**Table 2**
Preparation methods of the different catalysts. All the catalysts contain 5 wt% Pt. M (second metal): Ga or In.

| Catalyst designation | Preparation method | M (wt%) | M/Pt atomic ratio |
|---|---|---|---|
| Pt/CN-P<br>Pt/CV | (i) Conventional impregnation<br>(ii) Reductive treatment in $H_2$ flow at 350 °C for 3 h | – | – |
| PtGa(X wt%)/CN-P<br>PtGa(X wt%)/CV | (i) Successive impregnation<br>(ii) Reductive treatment in $H_2$ flow at 350 °C for 3 h | $X$ = 0.6, 1.8 or 3.12 | 0.33, 1 or 1.75, according to the corresponding value of $X$ |
| [PtGa(X wt%)/CN-P]-$N_2$<br>[PtGa(X wt%)/CV]-$N_2$ | (i) Successive impregnation<br>(ii) Reductive treatment in $H_2$ flow at 350 °C for 3 h<br>(iii) Thermal treatment in $N_2$ flow at 700 °C for 12 h | $X$ = 1.8 | 1 |
| PtIn(Y wt%)/CN-P<br>PtIn(Y wt%)/CV | (i) Successive impregnation<br>(ii) Reductive treatment in $H_2$ flow at 350 °C for 3 h | $Y$ = 0.97, 1.94, 2.5 or 2.95 | 0.33, 0.66, 0.85 or 1, according to the corresponding value of $Y$ |
| [PtIn(Y wt%)/CN-P]-$N_2$<br>[PtIn(Y wt%)/CV]-$N_2$ | (i) Successive impregnation<br>(ii) Reductive treatment in $H_2$ flow at 350 °C for 3 h<br>(iii) Thermal treatment in $N_2$ flow at 700 °C for 12 h | $Y$ = 2.5 | 0.85 |

a pass energy of 30 eV and a Mg anode operated at 100 W. The pressure of the analysis chamber was kept lower than $5 \times 10^{-8}$ mbar. Samples were previously reduced under $H_2$ at 350 °C for 3 h in a flow reactor and then they were introduced in the equipment and reduced "in situ" with $H_2$ at 350 °C for 1 h. Peak areas and binding energies (BE) values were estimated by fitting the curves with combination of Lorentzian–Gaussian curves of variable proportion using the CasaXPS Peak-fit software version 1.2. In order to accurately determine the peak position, the BE values of the energy levels of the corresponding atoms species were referenced to the C 1s (BE at 284.6 eV). Besides, to correctly fit the Pt 4f spectra of the different catalysts, the corresponding deconvolutions were performed assuming an intensity ratio of Pt $4f_{7/2}$ to Pt $4f_{5/2}$ of 1:0.75, and a separation between the Pt 4f doublet signals of 3.36 eV [26,27].

TEM measurements were carried out on a JEOL 100CX microscope with a nominal resolution of 0.6 nm, operated with an acceleration voltage of 100 kV, and magnification ranges of 80 000× and 100 000×. The samples were prepared by grinding, suspending and sonicating them in ethanol, and putting a drop of the suspension on a carbon copper grid. After evaporation of the solvent, the specimens were introduced into the microscope column. For each catalyst, a very important number of Pt particles (about 150) were observed and the distribution curves of particle sizes were done. The mean metallic particle diameter ($d$) was calculated as: $d = \frac{\sum n_i d_i}{\sum n_i}$, where $n_i$ is the number of particles of diameter $d_i$.

The different catalysts were tested in the citral hydrogenation at 70 °C and atmospheric pressure in a discontinuous glass reactor with a device for sampling the reaction products. In each experiment, 0.3 mL of citral (Aldrich, 61% cis and 36% trans) were hydrogenated by using 0.300 g of catalyst and 30 mL of solvent (2-propanol). The reaction mixture was stirred at 1400 rpm. It must be noted that from previous experiments, diffusional limitations were found to be absent under these conditions [28]. Prior to the reaction, catalysts were reduced "in-situ" under flowing $H_2$ at 350 °C for 3 h, and then they were cooled down to the reaction temperature. The reaction products were analyzed in a GC system coupled to a capillar column (Supelcowax 10 M) and using a FID detector. All products were identified by using gas chromatography standards, except for 3,7-dimethyloctanal and other secondary products. These last products were identified by gas chromatography–mass spectrometry (GC–MS) technique. The catalytic activity was defined as the sum of percentages of citral converted into different products. The selectivity to a given product ($i$) was calculated as the ratio between the amount of product ($i$) and the total amounts of products. Fig. 1 shows the scheme of the citral hydrogenation reaction and the main obtained products.

## 3. Results and discussion

### 3.1. Characterization of the catalysts

#### 3.1.1. Test reactions of the metallic phase and $H_2$ chemisorption

Tables 3 and 4 show the values of the initial rates of cyclohexane dehydrogenation ($R^0_{CH}$) and cyclopentane hydrogenolysis ($R^0_{CP}$) for PtGa and PtIn bimetallic series. The values of activation energy in CHD ($Ea_{CH}$) and of the $H_2$ chemisorption capacity ($H$) are also included.

In the case of PtGa bimetallic catalysts over both supports (Table 3), it can be observed that the initial reaction rates (of CHD and CPH) and chemisorption capacities significantly decrease when increasing the Ga loading. In fact, the highest Ga loading shows the lowest CHD and CPH initial activities with a decrease of one order of magnitude in the chemisorption capacity with respect to the monometallic sample. However, there is an increase in the initial reaction rate of CHD for PtGa(0.6 wt%)/CV catalyst while the same value for PtGa(0.6 wt%)/CN-P catalyst slightly decreases with respect to the corresponding monometallic catalyst. It must be pointed out that the CPH is a structure-sensitive reaction carried out on ensembles of a certain number of active atoms. Thus, the addition of a promoter to Pt (active metal) can break these ensembles and diminishes the CPH reaction rate. Hence, the marked decrease in the CPH initial reaction rates could be evidence of strong geometric effects, like blocking and dilution, taking place. The activation energy values in CHD show a slight decrease for PtGa bimetallic catalysts with respect to the monometallic ones. The CHD is a structure-insensitive reaction, which is carried out on one surface active atom of the catalyst. Hence the modification in the activation energy values is probably due to an electronic effect [14].

In the case of PtIn bimetallic catalysts over CV and CN-P (Table 4) it can be observed that both series show similar behaviors as the In content increases. Regarding CPH results, the addition of In to Pt in both supports produces a significant decrease of the initial reaction rate up to 100 times for the catalyst with the highest In loading compared with the monometallic catalyst. CHD values show another tendency. Thus, the initial CHD reaction rate is similar to those of the corresponding monometallic ones for the lower In content, while the catalysts with higher In loadings show lower values than those of the corresponding monometallic catalysts. This decrease reaches up to 85% for the highest In loading. The activation energy values in CHD show a decrease with In addition to Pt, but it is important to remark that this behavior is not a function of the In content because the $Ea_{CH}$ values remain practically the same for all PtIn catalysts. Table 4 also shows $H_2$ chemisorption capacities which largely decrease when increasing In amounts are added to Pt in both

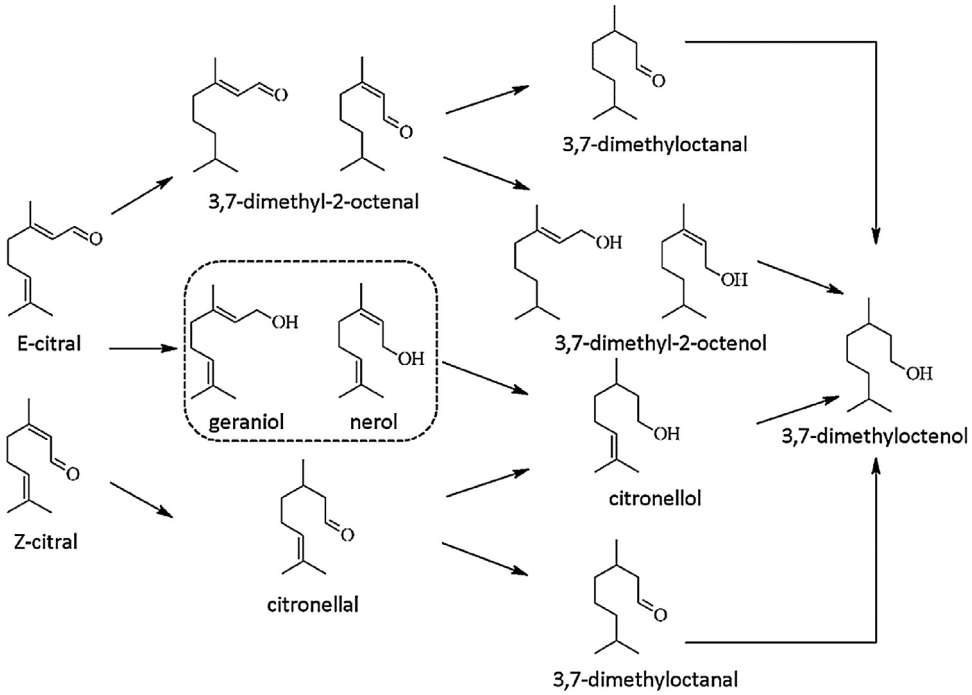


**Fig. 1.** The pathways of citral hydrogenation.

**Table 3**
Initial reaction rates of CHD ($R^0_{CH}$) and CPH ($R^0_{CP}$), activation energy in CHD ($Ea_{CH}$) and $H_2$ chemisorption capacity ($H$) for PtGa catalysts.

| Catalyst | $R^0_{CH}$ (mol/h gPt) | $Ea_{CH}$ (kcal/mol) | $R^0_{CP}$ (mol/h gPt) | $H$ (mol/g cat) |
|---|---|---|---|---|
| Pt/CN-P | 1.78 | 41 | 8.87 | 38.05[a] ($D$ = 29.8%) |
| PtGa(0.6 wt%)/CN-P | 1.15 | 35 | 0.36 | n.m. |
| PtGa(1.8 wt%)/CN-P | 0.22 | 37 | 0.09 | 0.62 |
| PtGa(3.12 wt%)/CN-P | <0.1 | n.m. | n.d. | <0.5 |
| [PtGa(1.8 wt%)/CN-P]-$N_2$ | <0.1 | n.m. | 0.08 | 0.97 |
| Pt/CV | 0.71 | 40 | 6.30 | 34.75[a] ($D$ = 27.2%) |
| PtGa(0.6 wt%)/CV | 1.70 | 30 | 0.15 | n.m. |
| PtGa(1.8 wt%)/CV | 0.45 | 36 | 0.08 | 2.04 |
| PtGa(3.12 wt%)/CV | <0.1 | n.m. | n.d. | <0.5 |
| [PtGa(1.8 wt%)/CV]-$N_2$ | <0.1 | n.m. | 0.07 | 0.97 |

n.d., not detected; n.m., not measured.
[a] $D$ = Pt dispersion (%).

**Table 4**
Initial reaction rates of CHD ($R_{CH}{}^0$) and CPH ($R_{CP}{}^0$), activation energy in CHD ($Ea_{CH}$) and $H_2$ chemisorption capacity ($H$) for PtIn catalysts.

| Catalyst | $R^0_{CH}$ (mol/h Pt) | $Ea_{CH}$ (kcal/mol) | $R^0_{CP}$ (mol/h gPt) | $H$ (mol/g cat) |
|---|---|---|---|---|
| Pt/CN-P | 1.78 | 41 | 8.87 | 38.05[a] ($D$ = 29.8%) |
| PtIn(0.97 wt%)/CN-P | 1.87 | 35 | 0.15 | 2.20 |
| PtIn(1.94 wt%)/CN-P | 1.41 | 36 | 0.24 | 4.00 |
| PtIn(2.5 wt%)/CN-P | 0.82 | 38 | 0.07 | 3.00 |
| PtIn(2.95 wt%)/CN-P | 0.25 | 38 | 0.06 | 1.62 |
| [PtIn(2.5 wt%)/CN-P]-$N_2$ | <0.1 | n.m. | 0.06 | <0.1 |
| Pt/CV | 0.71 | 40 | 6.30 | 34.75[a] ($D$ = 27.2%) |
| PtIn(0.97 wt%)/CV | 1.06 | 33 | 0.10 | 5.49 |
| PtIn(1.94 wt%)/CV | 0.64 | 32 | 0.15 | 1.71 |
| PtIn(2.5 wt%)/CV | 0.43 | 35 | 0.14 | 2.66 |
| PtIn(2.95 wt%)/CV | <0.1 | n.m. | n.m. | n.d. |
| [PtIn(2.5 wt%)/CV]-$N_2$ | <0.1 | n.m. | 0.06 | n.m. |

n.d., not detected; n.m., not measured.
[a] $D$ = Pt dispersion (%).

catalytic series (up to 95% for 2.95 wt% In load). PtIn(1.94 wt%)/CN-P shows a hydrogen chemisorption value slightly higher than the catalyst with 0.97 wt% In loading. In conclusion, the CHD results indicate the presence of blocking and electronic effects in PtIn catalysts. The CPH results show a great diminution of the number of the necessary ensembles for this reaction, which is due to the presence of dilution of Pt by In. Hence, blocking or dilution effects of Pt by In could be related to the presence of both ionic and zerovalent In species, which could be intercalated among Pt atoms blocking them in different ways. Besides, the formation of PtIn alloys could be present producing an electronic modification of the metallic phase.

Tables 3 and 4 also show the CHD and CPH results of the following catalysts: [PtGa(1.8 wt%)/CN-P]-$N_2$, [PtGa(1.8 wt%)/CV]-$N_2$, [PtIn(2.5 wt%)/CN-P]-$N_2$ and [PtIn(2.5 wt%)/CV]-$N_2$, which were submitted to a thermal treatment under nitrogen flow at 700 °C for 12 h after the reduction treatment ($H_2$, 350 °C, 3 h). The nitrogen thermal treatment was carried out in order to modify the concentration of functional groups and to induce a possible sinterization of the metallic phase. Therefore, it is expected a decrease of the initial activities in CHD and CPH compared with the corresponding catalysts without thermal treatment. It must be considered that the number of available surface Pt atoms are slightly lower in these catalysts treated with nitrogen (see XPS results) as well as the number of the necessary ensembles to carry out the hydrogenolysis reaction. Moreover, the hydrogen chemisorption values markedly decrease for all $N_2$-treated catalysts, which indicates a strong modification of the surface structure after the thermal treatment.

### 3.1.2. TPR profiles

Fig. 2 shows TPR profiles of PtGa and PtIn systems supported on CN-P and CV, the ones of the supports and of the monometallic catalysts as well. Besides, for the sake of comparison, TPR profiles of PtGa catalysts previously reduced at 350 °C for 3 h in flowing hydrogen and Ga ones reduced at 550 °C for 3 h in hydrogen flow were also included.

TPRs of both supports (Fig. 2) show a small and wide hydrogen consumption zone over 450 °C caused by the decomposition of functional groups which desorb CO, leaving unsaturated sites that react with hydrogen at high temperatures [29–31]. From a previous TPD characterization of CV [9], no desorption of acid groups were found, so the hydrogen consumption in the TPR profile (Fig. 2b and d) could be due to other sites (weak basic or acid ones) which do not desorb CO, but they could be interacting with hydrogen at high temperatures [32,33]. This behavior is probably due to the fact that $H_2$ can facilitate the decomposition of oxygen surface groups (C[O]) which release CO. In this way, the desorption of weak surface oxygen groups would leave new reactive sites ($C_f$) over the carbon surface which could interact with hydrogen at high temperatures [30].

Pt, Pt/CN-P and Pt/CV TPR profiles show a $H_2$ consumption peak at about 180–200 °C that corresponds to the reduction of the metallic complex to zerovalent state [34–36]. Hydrogen consumption zones between 375 and 550 °C in the monometallic catalysts correspond to the decomposition of functional groups of the support at lower temperatures catalyzed by Pt.

Fig. 2a and b shows the TPR profiles of the PtGa catalysts supported on CN-P and CV, respectively. For both series, the Pt reduction peak (150–200 °C) is shifted to lower temperatures compared with the monometallic catalyst, this shift being higher for the catalyst with the lowest Ga loading (0.6 wt%). The small shoulder at the end of the Pt reduction peak for PtGa(0.6 wt%)/CN-P and PtGa(0.6 wt%)/CV could be caused either by a Ga co-reduction catalyzed by Pt or by the reduction of different species formed from the interaction of both metals. All the catalysts of the series show a wide hydrogen consumption zone between 250 and 700 °C. Both bimetallic catalysts with the lowest Ga loading show a hydrogen desorption zone at temperatures above 600 °C probably due to hydrogen weakly bound to the support which is desorbed at this temperature. The other bimetallic catalysts also display this desorption zone but at higher temperatures.

For the Ga(1.8 wt%)/CN-P catalyst, two small reduction zones at high temperatures are observed: a wide peak (400–650 °C) and a very small shoulder above 700 °C. For Ga(1.8 wt%)/CV catalyst, a wide peak (300–750 °C) is observed that would correspond to the reduction of different Ga species. These differences could be attributed to the presence of different Ga species on each support. By comparing with the profiles of unreduced catalysts, the TPRs of PtGa(1.8 wt%)/CN-P red. 350 °C and PtGa(1.8 wt%)/CV red. 350 °C catalysts show that an important Ga fraction would be simultaneously reduced with Pt at 350 °C.

Summarizing, PtGa catalysts show a reduction peak at the same zone where the Pt reduction peak is located in the monometallic catalysts. In both series, hydrogen consumption in the Pt reduction zone is higher at higher Ga loadings which could be related with a catalytic Pt effect over the Ga reduction. These results will be related with the corresponding XPS ones.

Fig. 2c and d shows the TPR profiles of PtIn series. For the monometallic In catalysts (In(2.5 wt%)/CN-P and In(2.5 wt%)/CV), there is a hydrogen consumption zone from 250 °C to 750 °C, overlapping at high temperatures with the hydrogen consumption zone of the support. PtIn catalysts show a shift of the Pt reduction peak (with respect to the corresponding monometallic ones) to lower temperatures (from 180–200 °C to 140–150 °C) over both supports and for all the In loadings. It is observed that the higher the loading, the lower the reduction temperature. Besides, the intensities of the Pt reduction peak for the bimetallic catalysts are higher than those of the monometallic ones, this peak also getting narrower when increasing the In loading. At high temperatures (more than 670 °C), bimetallic catalysts also display a hydrogen desorption zone similarly to the PtGa series.

In conclusion, TPR profiles indicate that Pt and In fractions would be co-reduced, probably forming PtIn alloyed phases, this effect being similar for both PtIn series. Thus, it is possible that the adsorbed and then dissociated hydrogen (over the Pt particles or over the reactive sites created by the decomposition of the functional groups) could reduce the ionic In species placed over the support or near metallic Pt. Most of hydrogen would be dissociated by metallic Pt in PtIn systems, and then it could reduce In and functional groups of the support. This fact will be confirmed by XPS measurements.

### 3.1.3. XPS characterization

Figs. 3 and 4 show XPS spectra of Pt 4f, Ga 2p and In 3d of some PtGa and PtIn catalysts supported on CN-P and CV. Tables 5 and 6 show the binding energy values (BE) of Pt $4f_{7/2}$, Ga 2p, Ga 3d and In $3d_{5/2}$ levels, the percentages of oxidized and reduced species and the Pt/C, Ga/Pt and In/Pt atomic ratios.

The asymmetry shown by Pt 4f level between 76 and 80 eV would indicate the presence of both ionic Pt(II) or Pt(IV) species, that could be due to chloride species which remain unreduced in the final catalyst. Besides, an important metallic Pt signal between 71 and 72 eV is obtained. This signal is due to Pt that could form stable species by interacting with surface oxygenated groups and other support sites [37,38].

Table 5 shows the deconvolution of Pt 4f signal in three doublets for each species ($Pt^0$, $Pt^{+2}$, $Pt^{+4}$). Both Ga 2p and 3d levels were scanned to verify the proportion of reduced and oxidized species. Fig. 3 shows the Ga 2p level, meanwhile the percentages of each species are shown in Table 5. The Ga 3d BE are 19.05–19.51 eV for the zerovalent state and 21.05 and 21.51 eV for the oxidized species [39]. Ga 2p BE are placed at 1117.03–1117.47 eV for the zerovalent state and at 1118.26–1118.67 eV for the oxidized ones [17].

The percentages of metallic Pt in PtGa catalyst series, shown in Table 5, are 10–20% higher than the corresponding value of the monometallic ones. These values are not significantly modified neither by the nitrogen thermal treatment nor by the Ga loading. An important fraction of Ga is present as zerovalent state for the catalysts supported over both materials, CN-P and CV. The high proportion of Pt and Ga in zerovalent state would promote the formation of alloyed species [40].

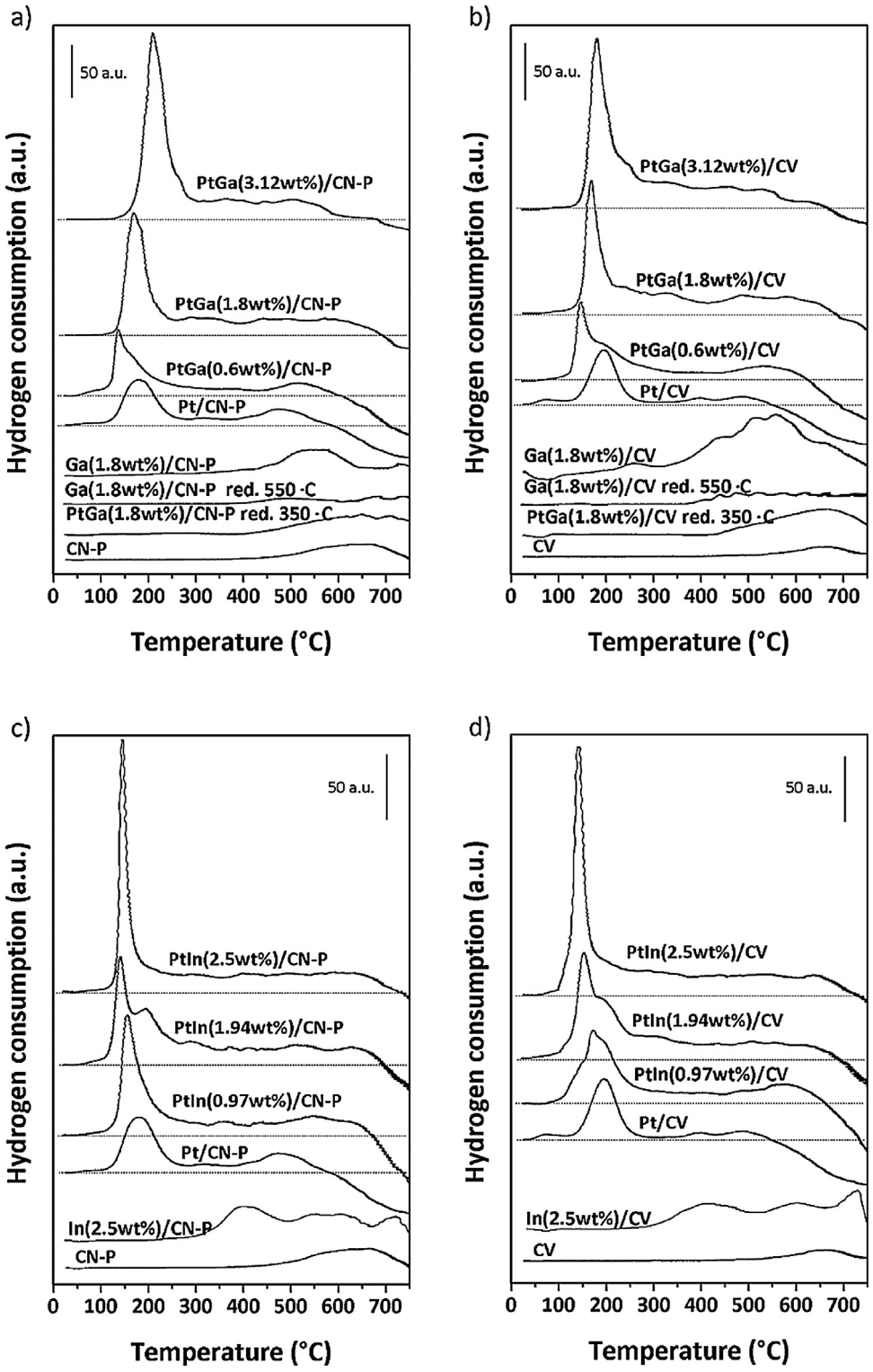


**Fig. 2.** TPR profiles for the different bimetallic catalytic series: (a) PtGa/CN-P, (b) PtGa/CV, (c) PtIn/CN-P, and (d) PtIn/CV.

The Pt/C surface atomic ratio, which is considered as an estimation of surface Pt atoms, decreases when Ga loading increases for both catalytic series. In the case of the nitrogen treated catalysts, no important changes in the Pt/C ratio were observed, since these catalysts would probably resist the sintering process by the high temperature treatment. From Ga/Pt ratios it could be seen a very noticeable surface Ga enrichment for all the catalysts, this fact being more important for nitrogen-treated PtGa/CN-P ones. Thus, Pt/C and Ga/Pt ratios would indicate an important geometric effect of Ga that produce blocking more than dilution of the Pt metallic surface.

The XPS data of PtIn catalysts is quite different. Fig. 4 shows the deconvolutions of the corresponding In $3d_{5/2}$ spectra in two peaks: one at low BE (4443–4445 eV), and another one at higher BE (4459–4465 eV). The first peak corresponds to zerovalent In, and the other one to $In^{+1/+3}$ species. $In^{+1}$ and $In^{+3}$ peaks cannot

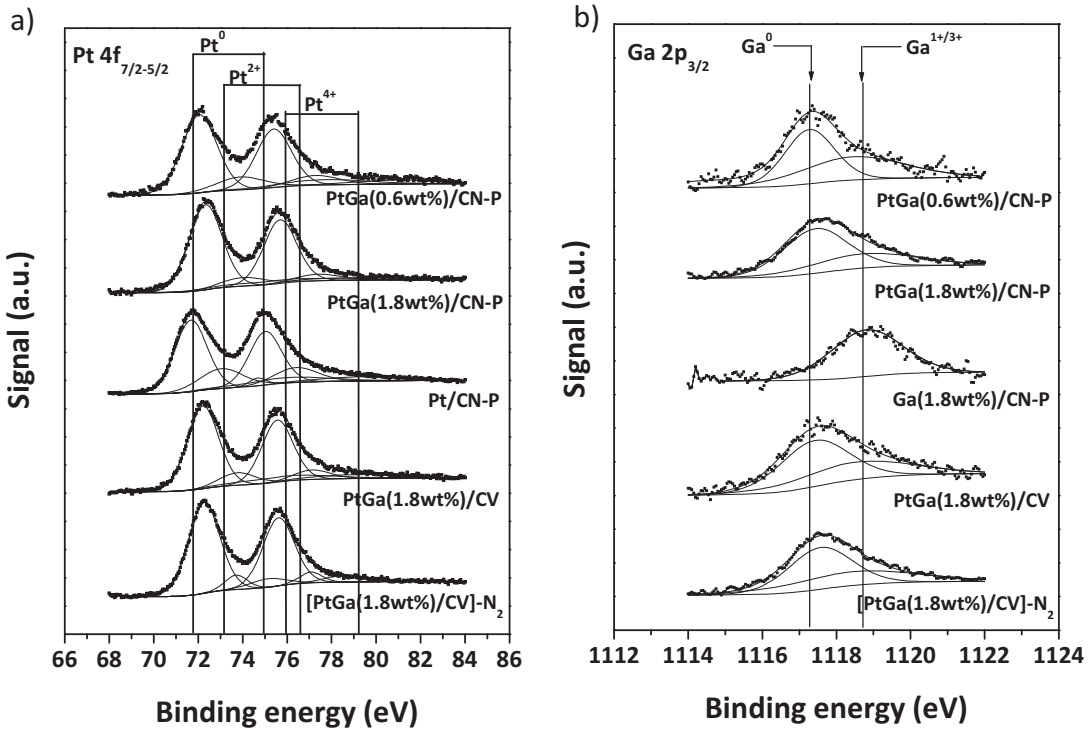


**Fig. 3.** Pt and Ga XPS profiles for the PtGa catalytic series: (a) Pt 4f level and (b) Ga 2p level.

be distinguished since their BE are very similar [16]. From Table 6 it is observed that the In addition to Pt catalysts increases the Pt reducibility from 64% for the monometallic catalyst up to 79–80% for the bimetallic one with the highest loading. Besides, the metallic In percentage increases from 80 to about 90% when the promoter loading increases for both catalytic series.

The Pt/C atomic ratio of the bimetallic catalysts decreases respect to the monometallic ones, thus indicating the presence of a geometric effect (blocking or dilution) caused by the promoter addition. It can be seen a slight increase of this ratio when the In loading increases in both series, this fact could be a consequence of a rearrangement of the metallic phases with the subsequent increase of surface Pt sites. Besides, considering that the In/Pt surface atomic ratio for both catalytic series is similar to the In/Pt nominal ratio (see Table 2), there would be no evidence of In surface enrichment. In conclusion, an electronic modification of the metallic phase due to

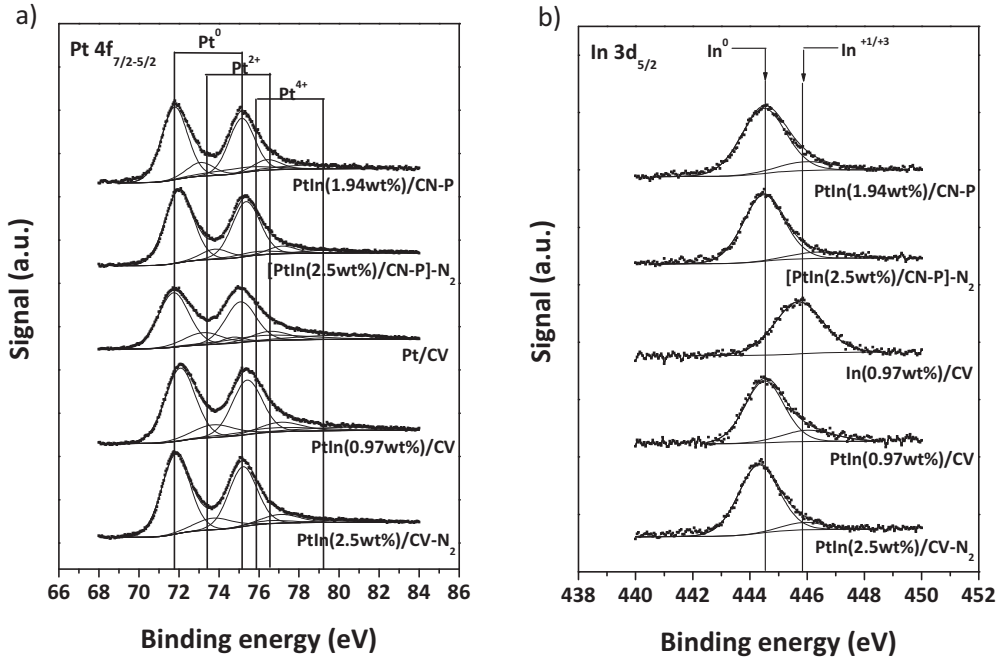


**Fig. 4.** Pt and In XPS profiles for the PtIn catalytic series: (a) Pt 4f level and (b) In 3d level.

**Table 5**
XPS results of the PtGa catalytic series supported on CN-P and CV.

| Catalysts | Atomic ratio | | Pt $4f_{7/2}$ level | | | Ga 2p level | | | Ga 3d level | | |
|---|---|---|---|---|---|---|---|---|---|---|---|
| | Pt/C | Ga/Pt | BE (eV) | Species | Atomic% | BE (eV) | Species | Atomic% | BE (eV) | Species | Atomic% |
| Pt/CN-P | 0.60 | – | 71.67 | $Pt^0$ | 63.6 | – | – | – | – | – | – |
| | | | 73.06 | $Pt^{+2}$ | 23.6 | | | | | | |
| | | | 75.95 | $Pt^{+4}$ | 12.8 | | | | | | |
| PtGa(0.6 wt%)/CN-P | 0.43 | 4.04 | 71.85 | $Pt^0$ | 72.1 | 1117.07 | $Ga^0$ | 52.9 | 19.15 | $Ga^0$ | 51.7 |
| | | | 73.72 | $Pt^{+2}$ | 15.9 | 1118.26 | $Ga^{+1/+3}$ | 47.1 | 21.15 | $Ga^{+1/+3}$ | 48.3 |
| | | | 77.47 | $Pt^{+4}$ | 12.0 | | | | | | |
| PtGa(1.8 wt%)/CN-P | 0.39 | 4.68 | 72.03 | $Pt^0$ | 79.0 | 1117.14 | $Ga^0$ | 65.9 | 19.39 | $Ga^0$ | 64.6 |
| | | | 73.75 | $Pt^{+2}$ | 10.7 | 1118.44 | $Ga^{+1/+3}$ | 34.1 | 21.39 | $Ga^{+1/+3}$ | 35.4 |
| | | | 75.21 | $Pt^{+4}$ | 10.3 | | | | | | |
| [PtGa(1.8 wt%)/CN-P]-$N_2$ | 0.35 | 5.69 | 71.98 | $Pt^0$ | 80.0 | 1117.03 | $Ga^0$ | 59.3 | 19.19 | $Ga^0$ | 59.9 |
| | | | 73.56 | $Pt^{+2}$ | 15.0 | 1118.67 | $Ga^{+1/+3}$ | 40.7 | 21.19 | $Ga^{+1/+3}$ | 40.1 |
| | | | 75.79 | $Pt^{+4}$ | 5.0 | | | | | | |
| Pt/VC | 0.74 | – | 71.73 | $Pt^0$ | 64.8 | – | – | – | – | – | – |
| | | | 73.22 | $Pt^{+2}$ | 17.8 | | | | | | |
| | | | 76.41 | $Pt^{+4}$ | 17.5 | | | | | | |
| PtGa(0.6 wt%)/CV | 0.34 | 4.01 | 72.05 | $Pt^0$ | 72.1 | 1117.13 | $Ga^0$ | 56.4 | 19.05 | $Ga^0$ | 55.5 |
| | | | 73.91 | $Pt^{+2}$ | 15.9 | 1118.55 | $Ga^{+1/+3}$ | 43.6 | 21.05 | $Ga^{+1/+3}$ | 44.5 |
| | | | 76.43 | $Pt^{+4}$ | 12.0 | | | | | | |
| PtGa(1.8 wt%)/CV | 0.44 | 4.21 | 72.01 | $Pt^0$ | 74.0 | 1117.21 | $Ga^0$ | 61.5 | 19.50 | $Ga^0$ | 60.8 |
| | | | 73.57 | $Pt^{+2}$ | 13.0 | 1118.32 | $Ga^{+1/+3}$ | 38.5 | 21.50 | $Ga^{+1/+3}$ | 39.2 |
| | | | 75.61 | $Pt^{+4}$ | 13.0 | | | | | | |
| [PtGa(1.8 wt%)/CV]-$N_2$ | 0.55 | 3.65 | 72.17 | $Pt^0$ | 82.1 | 1117.47 | $Ga^0$ | 60.1 | 19.51 | $Ga^0$ | 60.6 |
| | | | 73.61 | $Pt^{+2}$ | 9.2 | 1118.35 | $Ga^{+1/+3}$ | 39.9 | 21.51 | $Ga^{+1/+3}$ | 39.4 |
| | | | 75.04 | $Pt^{+4}$ | 8.7 | | | | | | |

**Table 6**
XPS results of the PtIn catalytic series supported on CN-P and CV.

| Catalysts | Atomic ratio | | Pt $4f_{7/2}$ level | | | In $3d_{5/2}$ level | | |
|---|---|---|---|---|---|---|---|---|
| | Pt/C | In/Pt | BE (eV) | Species | Atomic % | BE (eV) | Species | Atomic % |
| Pt/CN-P | 0.60 | – | 71.67 | $Pt^0$ | 63.6 | – | – | – |
| | | | 73.06 | $Pt^{+2}$ | 23.6 | | | |
| | | | 75.95 | $Pt^{+4}$ | 12.8 | | | |
| PtIn(1.94 wt%)/CN-P | 0.38 | 0.83 | 71.69 | $Pt^0$ | 69.6 | 444.4 | $In^0$ | 86.1 |
| | | | 73.00 | $Pt^{+2}$ | 19.8 | 446.2 | $In^{+1/+3}$ | 13.9 |
| | | | 75.44 | $Pt^{+4}$ | 10.6 | | | |
| PtIn(2.5 wt%)/CN-P | 0.45 | 0.81 | 71.80 | $Pt^0$ | 79.8 | 444.5 | $In^0$ | 89.3 |
| | | | 73.46 | $Pt^{+2}$ | 11.1 | 446.3 | $In^{+1/+3}$ | 10.7 |
| | | | 75.80 | $Pt^{+4}$ | 9.1 | | | |
| [PtIn(1.94 wt%)/CN-P]-$N_2$ | 0.35 | 0.49 | 71.80 | $Pt^0$ | 76.9 | 444.3 | $In^0$ | 90.0 |
| | | | 73.48 | $Pt^{+2}$ | 15.7 | 446.1 | $In^{+1/+3}$ | 10.0 |
| | | | 76.24 | $Pt^{+4}$ | 7.4 | | | |
| [PtIn(2.5 wt%)/CN-P]-$N_2$ | 0.45 | 0.59 | 71.90 | $Pt^0$ | 82.1 | 444.4 | $In^0$ | 89.4 |
| | | | 73.71 | $Pt^{+2}$ | 11.3 | 446.3 | $In^{+1/+3}$ | 10.6 |
| | | | 75.82 | $Pt^{+4}$ | 6.6 | | | |
| Pt/VC | 0.74 | – | 71.73 | $Pt^0$ | 64.8 | – | – | – |
| | | | 73.22 | $Pt^{+2}$ | 17.8 | | | |
| | | | 76.41 | $Pt^{+4}$ | 17.5 | | | |
| PtIn(0.97 wt%)/CV | 0.43 | 0.33 | 71.96 | $Pt^0$ | 70.9 | 444.4 | $In^0$ | 80.7 |
| | | | 73.65 | $Pt^{+2}$ | 17.2 | 446.0 | $In^{+1/+3}$ | 19.3 |
| | | | 76.71 | $Pt^{+4}$ | 11.9 | | | |
| PtIn(1.94 wt%)/CV | 0.57 | 0.63 | 71.83 | $Pt^0$ | 74.8 | 444.3 | $In^0$ | 85.8 |
| | | | 73.42 | $Pt^{+2}$ | 15.8 | 446.1 | $In^{+1/+3}$ | 14.2 |
| | | | 76.60 | $Pt^{+4}$ | 9.4 | | | |
| PtIn(2.5 wt%)/CV | 0.62 | 0.70 | 71.82 | $Pt^0$ | 79.0 | 444.5 | $In^0$ | 90.4 |
| | | | 73.26 | $Pt^{+2}$ | 14.4 | 446.5 | $In^{+1/+3}$ | 9.6 |
| | | | 75.04 | $Pt^{+4}$ | 6.6 | | | |
| [PtIn(2.5 wt%)/CV]-$N_2$ | 0.56 | 0.48 | 71.76 | $Pt^0$ | 79.3 | 444.3 | $In^0$ | 90.1 |
| | | | 73.96 | $Pt^{+2}$ | 16.3 | 445.9 | $In^{+1/+3}$ | 9.9 |
| | | | 76.96 | $Pt^{+4}$ | 4.4 | | | |

an important proportion of alloyed PtIn species and also a geometric modification of the metallic phase caused by In species would be present.

Taking into account that the percentages of $Ga^0$ and $In^0$ species are high in bimetallic samples, while there are only Ga and In ionic species in the corresponding monometallic catalysts (see XPS results), there would be a high Pt–promoter interaction and in consequence a poor interaction between the promoters and the support. Hence, during the correduction observed in the TPR profiles of bimetallic catalysts, a metallic phase with high reducibilities of Pt and the promoters to zerovalent state takes place.

### 3.1.4. TEM determinations

Selected bimetallic catalysts were chosen to determine particle size distributions by TEM and to analyze the possible modifications of the particle diameter after $N_2$ thermal treatment. Fig. 5 shows the

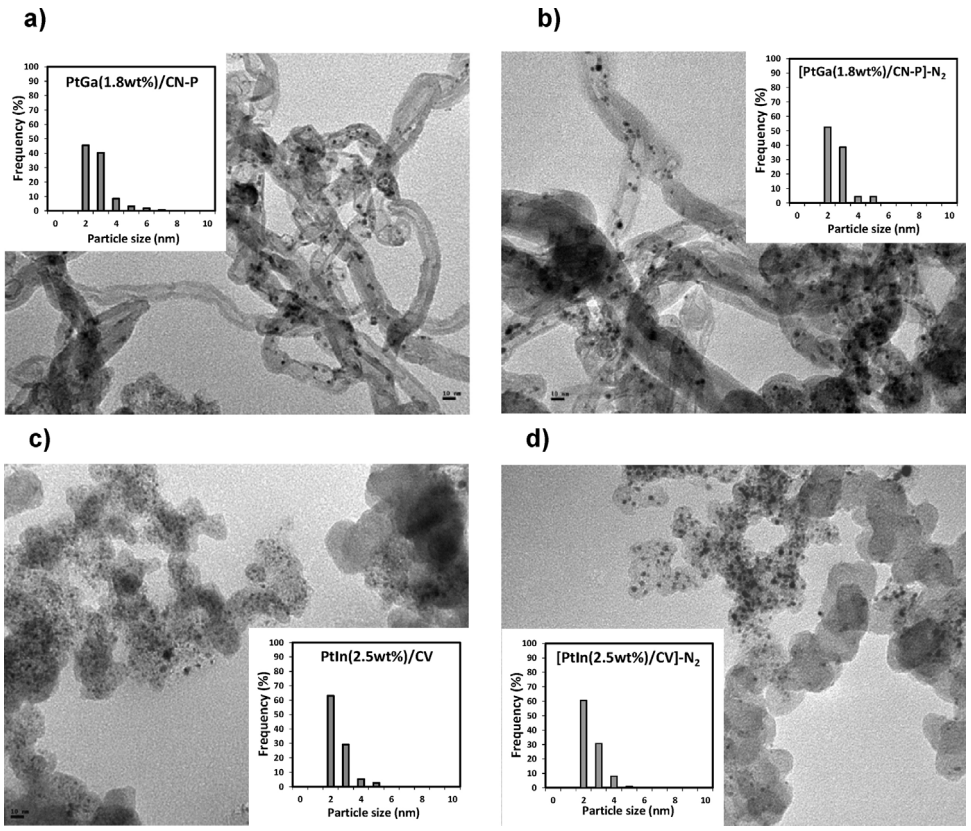


**Fig. 5.** TEM images and their distributions of particle diameters of: (a) PtGa(1.8 wt%)/CN-P, (b) [PtGa(1.8 wt%)/CN-P]-$N_2$, (c) PtIn(2.5 wt%)/CV, (d) [PtIn(2.5 wt%)/CV]-$N_2$. The magnification scale was 10 nm.

microphotographies together with the corresponding histograms of particle size distribution. For the catalysts before thermal treatment, the average diameters of Pt particles are very similar to the ones of the corresponding monometallic catalysts [21], 2.3 nm for PtGa(1.8 wt%)/CN-P and 2 nm for PtIn(2.5 wt%)/CV. However, from the histograms, it must be noted that the particle size distributions for both bimetallic catalysts are different. In this sense, the PtIn catalyst shows a narrower distribution than the PtGa one. In both cases, a high fraction of small particles are contributing to the total Pt area.

Catalysts with $N_2$ thermal treatment show no significant change in the average diameters of Pt particles compared to the untreated catalysts, 2.1 nm for [PtGa(1.8 wt%)/CN-P]-$N_2$ and 1.9 nm for [PtIn(2.5 wt%)/CV]-$N_2$. Besides, the particle size distributions appear to be rather similar to the distributions corresponding to the untreated catalysts. Hence, there would be a sintering resistance in these bimetallic catalysts. In a previous work, it was observed that monometallic Pt catalysts supported on carbon nanotubes were easily sintered during the $N_2$ thermal treatment [21], however in a bimetallic catalyst the promoter could be inhibiting the Pt migration.

#### 3.1.5. Characterization results discussion

From characterization results it can be concluded that the addition of Ga or In modifies the Pt metallic phase producing dilution, blocking effects and alloy formation.

The PtGa phase has similar behavior for both supports. TPR results show that the proportion of ionic and zerovalent species is quite similar for the PtGa catalytic series, thus indicating that similar metallic phases could be present. From XPS analysis, it was found a high fraction of $Ga^0$ species (also after $N_2$ treatment), an important Ga surface enrichment and probable Pt–Ga alloyed phases. Besides, the ionic fraction could have a promoting effect over the active metal and also it could be placed over the support blocking or hindering the acid sites of the supports.

PtIn catalysts supported over CN-P and CV show a promoting effect more pronounced than the PtGa catalytic series. Besides, the PtIn couple presents a similar catalytic behavior over both supports. From TPR results, a strong Pt–In interaction is observed. XPS results show a high fraction of In in zerovalent state (about 90%) for both CN-P and CV series. There could be an electronic modification of the metallic phase due to the presence of an important fraction of alloyed PtIn species although the promoting effect of In ionic species cannot be discarded.

The support influence on the metal–metal and metal–support interactions should be considered. Carbonaceous materials have an inert character that would reduce metal–support interaction [41] and ease the metal reducibility, thus favoring metal–metal interactions that would form alloyed phases [42,43].

### 3.2. Citral hydrogenation

Tables 7 and 8 show the required reaction times for reaching a citral conversion of 95% for bimetallic catalysts used in the citral hydrogenation. Fig. 6 shows the results of the citral conversion to all products as a function of the reaction time for each catalytic series: PtGa/CN-P, PtGa/CV, PtIn/CN-P and PtIn/CV. It must be noted that the activity was plotted up to the same reaction time (5 h). Fig. 7 displays the relative activity as a function of the Ga or In content for each catalytic series. The relative activity was defined as $\theta_{Pt}/\theta_{Pt-Promoter}$, being $\theta$ the required reaction time to reach 95% citral conversion for each catalyst. As it can be seen, the activities of the bimetallic catalysts PtGa/CN-P, PtIn/CN-P and PtGa/CV in general are higher than those of the monometallic ones, except for

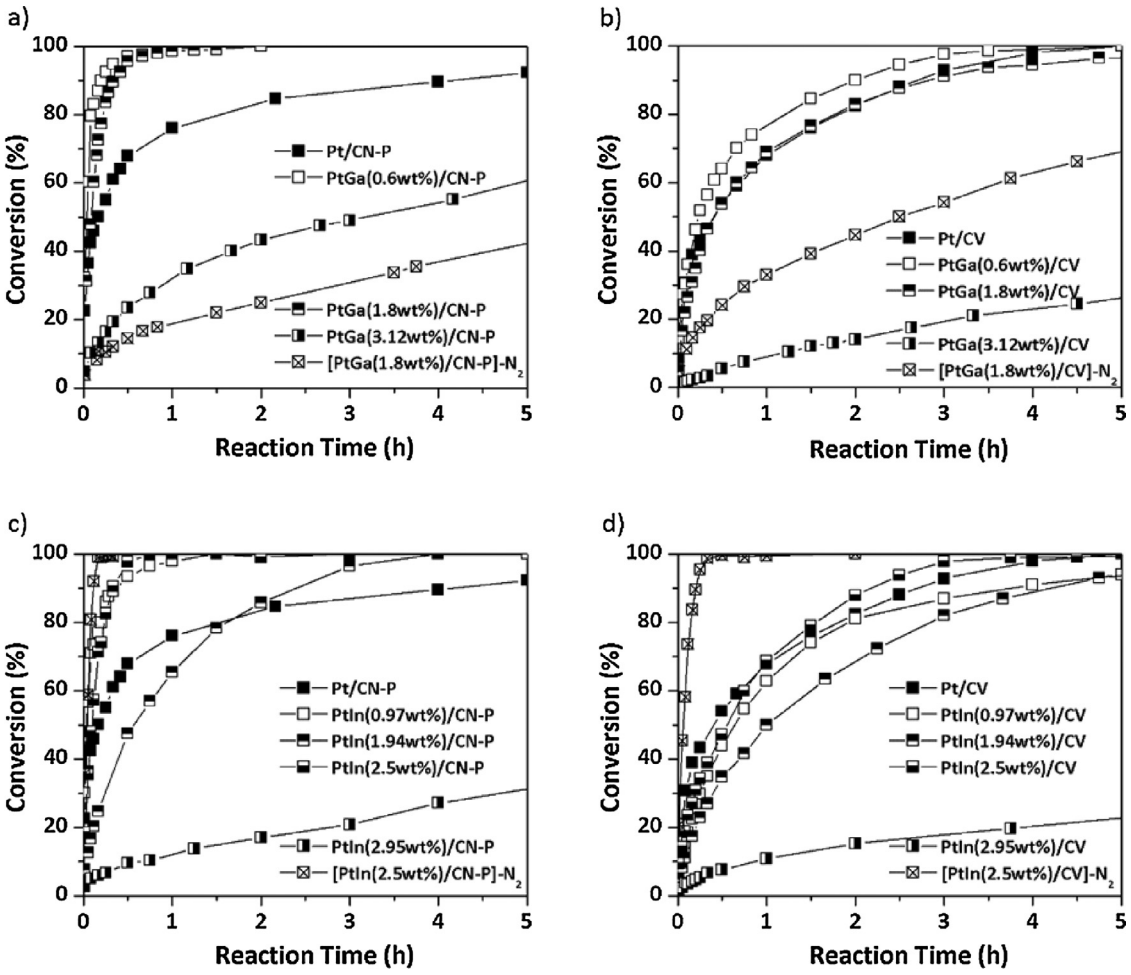


**Fig. 6.** Citral conversion as a function of the reaction time for the different bimetallic catalytic series: (a) PtGa/CN-P, (b) PtGa/CV, (c) PtIn/CN-P and (d) PtIn/CV.

**Table 7**
Reaction time reached at 95% citral conversion and the corresponding atomic ratio values for PtGa catalysts. All the catalysts contain 5 wt% Pt loading.

| Catalysts | Atomic ratio Ga/Pt | Reaction time (h) |
|---|---|---|
| Pvt/CN-P | – | 7.00 |
| PtGa(0.6 wt%)/CN-P | 0.33 | 0.12 |
| PtGa(1.8 wt%)/CN-P | 1.00 | 0.75 |
| PtGa(3.12 wt%)/CN-P | 1.75 | 15.00 |
| [PtGa(1.8 wt%)/CN-P]-$N_2$ | 1.00 | 12.00 **(66%)*** |
| Pt/CV | – | 3.30 |
| PtGa(0.6 wt%)/CV | 0.33 | 1.30 |
| PtGa(1.8 wt%)/CV | 1.00 | 2.35 |
| PtGa(3.12 wt%)/CV | 1.75 | 20.0 **(41%)*** |
| [PtGa(1.8 wt%)/CV]-$N_2$ | 1.00 | 5.50 |

* Values in bold and between brackets correspond to citral conversions lower than 95%.

**Table 8**
Reaction time reached at 95% citral conversion and the corresponding atomic ratio values for PtIn catalysts. All the catalysts contain 5 wt% Pt loading.

| Catalysts | Atomic ratio In/Pt | Reaction time (h) |
|---|---|---|
| Pt/CN-P | – | 7.00 |
| PtIn(0.97 wt%)/CN-P | 0.33 | 0.20 |
| PtIn(1.94 wt%)/CN-P | 0.66 | 0.40 |
| PtIn(2.5 wt%)/CN-P | 0.85 | 0.40 |
| PtIn(2.95 wt%)/CN-P | 1.00 | 13.0 **(68%)*** |
| [PtIn(2.5 wt%)/CN-P]-$N_2$ | 0.85 | 0.13 |
| Pt/CV | – | 3.30 |
| PtIn(0.97 wt%)/CV | 0.33 | 5.00 |
| PtIn(1.94 wt%)/CV | 0.66 | 5.50 |
| PtIn(2.5 wt%)/CV | 0.85 | 2.50 |
| PtIn(2.95 wt%)/CV | 1.00 | 10.0 **(33%)*** |
| [PtIn(2.5 wt%)/CV]-$N_2$ | 0.85 | 0.25 |

* Values in bold and between brackets correspond to citral conversions lower than 95%.

the highest promoter loadings. In this sense, the highest relative activities were found for PtGa(0.6 wt%)/CN-P (60 times higher) and for PtIn(0.97 wt%)/CN-P (35 times higher) compared to the corresponding Pt catalyst.

Nitrogen treated catalysts show opposite results (Tables 7 and 8). PtGa/CN-P-$N_2$ and PtGa/CV-$N_2$ catalysts show lower activities than the similar ones without treatment, e.g. the activity of [PtGa(1.8 wt%)/CN-P]-$N_2$ catalyst is 50 times lower than its partner. On the other hand, PtIn/CN-P-$N_2$ and PtIn/CV-$N_2$ catalysts show higher activities than their partners, the activity of [PtIn(2,5%)/CV]-$N_2$ being 10 times higher than the untreated catalyst. This can be explained taking into account that for PtGa catalysts the Pt/C surface atomic ratio decreases with the $N_2$ thermal treatment while the Ga/Pt ratio increases reaching important values. In the case of PtIn catalysts, the Pt/C ratio remains rather constant for both series and the In/Pt one decreases about 50% respect to the untreated ones. These modifications are evidences of the changes in the bimetallic phases as a consequence of the thermal treatment, mainly in the surface concentration of exposed Pt. Thus, the number of exposed Pt sites in PtIn series would be slightly modified by the thermal treatment. However, the effect of the promoter in PtGa catalysts would be the opposite. For PtGa

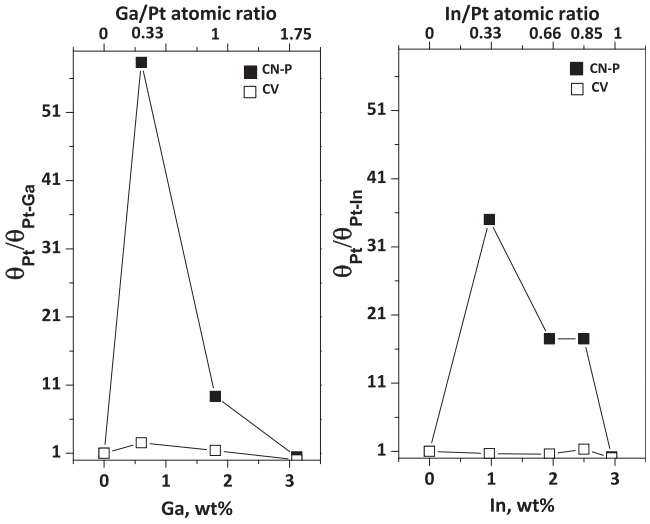


**Fig. 7.** Relative activity ($\theta_{Pt}/\theta_{Pt-Promoter}$) in citral hydrogenation versus Ga and In content for the different bimetallic catalysts.

series, the treatment would increase the blocking of Pt atoms due to the increase of surface Ga atoms, whereas in PtIn series the In/Pt surface atomic ratio decreases, thus indicating that there could be a rearrangement of metals. This fact could explain the high overall activity of PtIn catalysts. Besides, these effects can also be due to different metal–support interactions.

The promoters would be partially placed either in the vicinity of Pt atoms promoting selective hydrogenation reactions [7,6] or over the support reacting with surface acid groups, thus poisoning and hindering unwanted side reactions. The changes in the relative activity of bimetallic catalyst would depend on the oxidation state of the second metal. From XPS results of PtGa catalysts, about 30–40% Ga is in ionic state, which would inhibit side reactions improving the global hydrogenation rate, and the zerovalent fraction would be placed near the Pt probably forming alloyed phases that would produce a blocking effect rather than a dilution one, even though the influence of this last effect on the citral hydrogenation should not be discarded. The relative activity of PtIn/CN-P series reaches a maximum for the lowest In loading (Fig. 7). This fact would indicate that a low concentration of In would be enough to promote the hydrogenation reactions. The tendency observed for PtIn/CV series is different, thus indicating either a different exposition of the metallic phase or steric hindrance of the support.

Fig. 8 shows the selectivity values to different reaction products measured at three citral conversion levels (35, 65 and 95%) for PtGa and PtIn series supported on CN-P and CV. In order to highlight the selectivity toward the desirable products, Fig. 9 only shows the selectivity values to unsaturated alcohols (UA) for all the catalyst series. It can be observed that monometallic Pt catalysts are not selective to UA, showing low selectivity to the double conjugated bond, hence many secondary and undesirable products (BP) are obtained. Pt/CN-P catalyst is more selective to mono and bihydrogenated products (such as citronellal and citronellol) than Pt/CV one. To explain the differences in the selectivity, the nature of the supports must be considered, whose different surface oxygenated groups would modify the access of the molecule to be hydrogenated by the active sites [9]. The addition of the second metal increases the selectivity to UA [44,45] as it can be seen in Figs. 8 and 9.

For the PtGa series, the higher the Ga loading, the higher the selectivity to UA (Fig. 8a and b) and the lower the selectivities to side reactions even at the lowest Ga loading. However, there is an exception in the tendency corresponding to the highest Ga load (3.12 wt%). In this catalyst with a Ga/Pt atomic ratio higher than 1, Ga would block Pt particles. This effect would be much more evident on the catalyst over CV with a 40% decrease in the selectivity to UA with respect to the catalyst with 1.8 wt% of Ga loading. Besides, it must be noted that the selectivity to CAL also decreases even for the lowest Ga content with respect to the corresponding monometallic catalysts, but for the other Ga loadings this selectivity suffers a slight increase compared with the previous Ga load. Regarding COL selectivity, the higher the Ga content, the lower the selectivity values. Ionic Ga species over acid sites of the support [18] would inhibit side reactions and increase the selectivity to UA even at low Ga contents. Moreover, Ga has two promoter effects. On the one hand the Ga ionic species located in the neighboring of Pt particles would modify the metallic phase so the C=O hydrogenation is favored. On the other hand, $Ga^0$ could form alloyed phases with Pt in which Ga would have a slightly positive charge [46], this effect improving the polarization of the carbonyl group. Zerovalent Ga placed near Pt would be polarized by a shift of electronic density from Ga to Pt, in this way forming bimetallic sites that could interact with the carbonyl group [7,8]. Besides, the competition between C=C and C=O groups for the adsorption on the same site could be minimized, thus favoring C=O hydrogenation [8]. Thereby, the higher the Ga concentration over both supports, the higher the selectivity to UA and the lower the selectivity to CAL, since the adsorption of citral molecules would be modified by changing the surface chemistry of the active sites. In this sense the citral adsorption by the C=C bond would need a certain conformation of the adsorption sites, which differs from the ones needed for the citral adsorption by C=O bond. From XPS tests, very high Ga/Pt atomic surface ratios were obtained so it could be concluded that blocking and/or dilution effects of Ga particles over Pt are enough to prevent the hydrogenation of the double C=C bond, thus reducing the secondary products. The Ga effect over Pt is similar to the one showed by Fe analyzed in a previous work [9], but the promoting effect over selectivity to UA seems to be stronger than Fe in α,β-unsaturated aldehyde hydrogenation according to the literature [7]. It is worth noticing the high selectivity to UA showed by [PtGa(1.8 wt%)/CN-P]-$N_2$ catalyst respect to its partner without treatment, reaching a selectivity to UA of 98%. It seems that this catalyst tailors particle size and Pt–promoter interaction with the promoter concentration.

For PtIn catalysts, important improvements of the selectivity to UA for both series can be seen in Fig. 9, this value being about 70–80% for the lowest In loading (0.97 wt%) and 97% for the selected In loading (2.5 wt%) at 95% citral conversion. The promoting effect of In seems to be better than Ga one since the best catalytic performance of PtGa is achieved at Ga/Pt = 1. However, it is worth noticing that the best performance of PtIn is obtained for In/Pt < 1.

According to XPS results, most of the In is in zerovalent state for all PtIn catalysts. High In reducibilities were also found in the literature for trimetallic $MgAl_2O_4$ supported PtPbIn catalysts [16]. It is known that the ionic fraction of the second metal promotes the metallic phase to increase the selectivity to UA, poisons the acid sites of the support to inhibit side reactions and activates the carbonyl group by its polarization [47,48]. The carbonyl activation would depend on the monometallic catalyst promotion by ionic species with positive charge [7,49]. However, if it is considered that only 10% of the total In loading is available as ionic species to activate the carbonyl group, this would not be enough to completely explain the results. They could also be explained considering the presence of alloyed phases that would activate and hydrogenate the C=O group since there is an important fraction of zerovalent In (90%). The alloys and In ionic species would modify the metallic phase by dilution and/or blocking effects, thus reducing the double bond adsorption. It is known in the literature [50] that a typical promoter effect includes ionic species that selectively polarize the carbonyl group favoring its hydrogenation. However in the case of

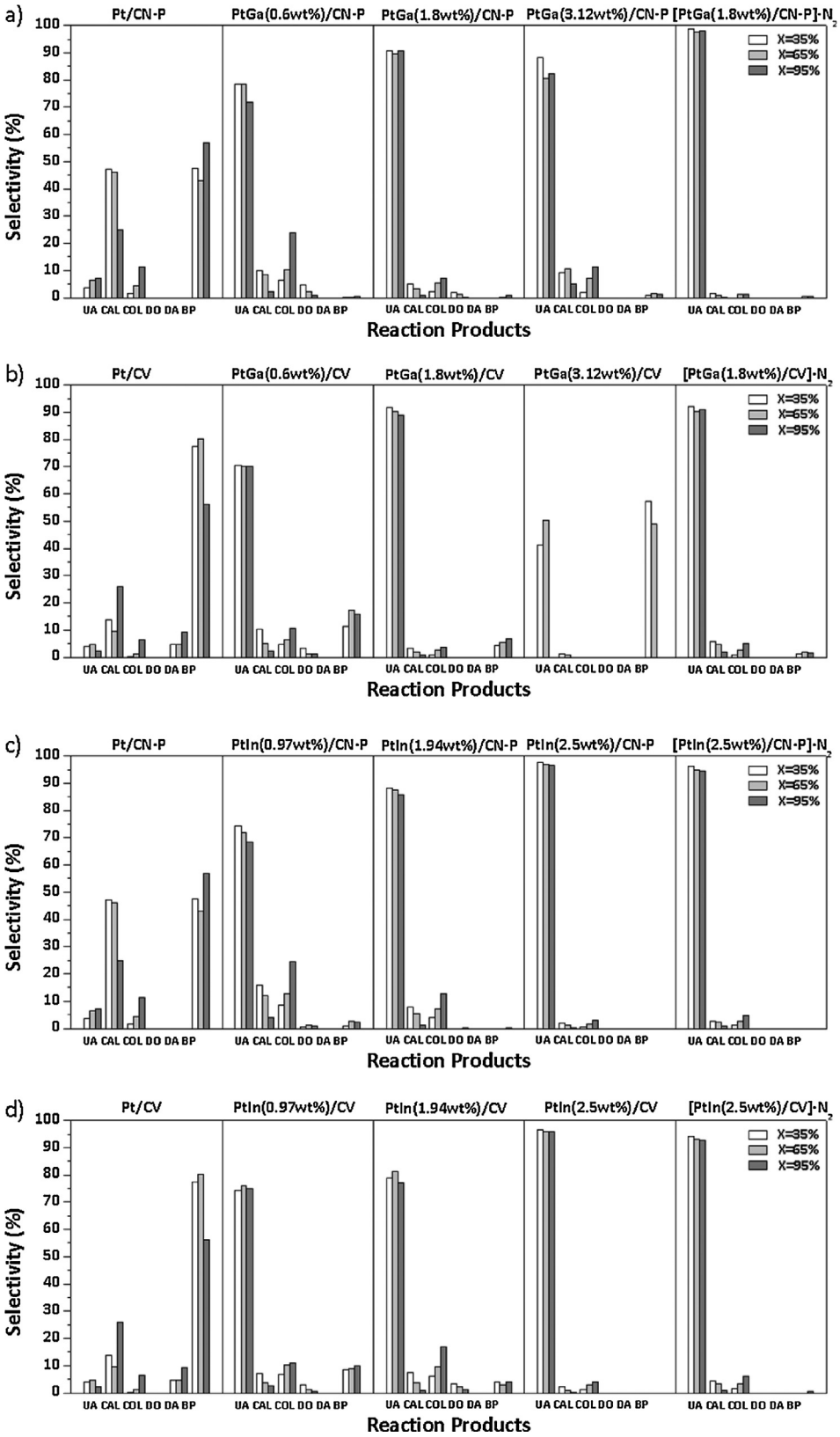


**Fig. 8.** Selectivities to different products measured at certain citral conversion levels (35, 65 and 95%) for the catalytic series: (a) PtGa/CN-P and (b) PtGa/CV, (c) PtIn/CN-P and (d) PtIn/CV. UA: unsaturated alcohols (geraniol and nerol), CAL: citronellal, COL: citronellol, DO: dimethyloctanol, DA: dimethyloctanal, BP: by products.

PtIn, the low concentration of ionic species could not explain all the promoting effect, as it happens with PtSn catalysts previously studied [9]. It should be noted that zerovalent In cannot hydrogenate double bonds by itself [51]. Although it was found in the literature evidences of the presence of alloyed phases in PtIn catalysts [16,17,51], no bibliographic information about the influence of PtIn alloyed species on the selectivity to UA in the α,β-unsaturated aldehydes hydrogenation was found. Hence, some hypothesis could be

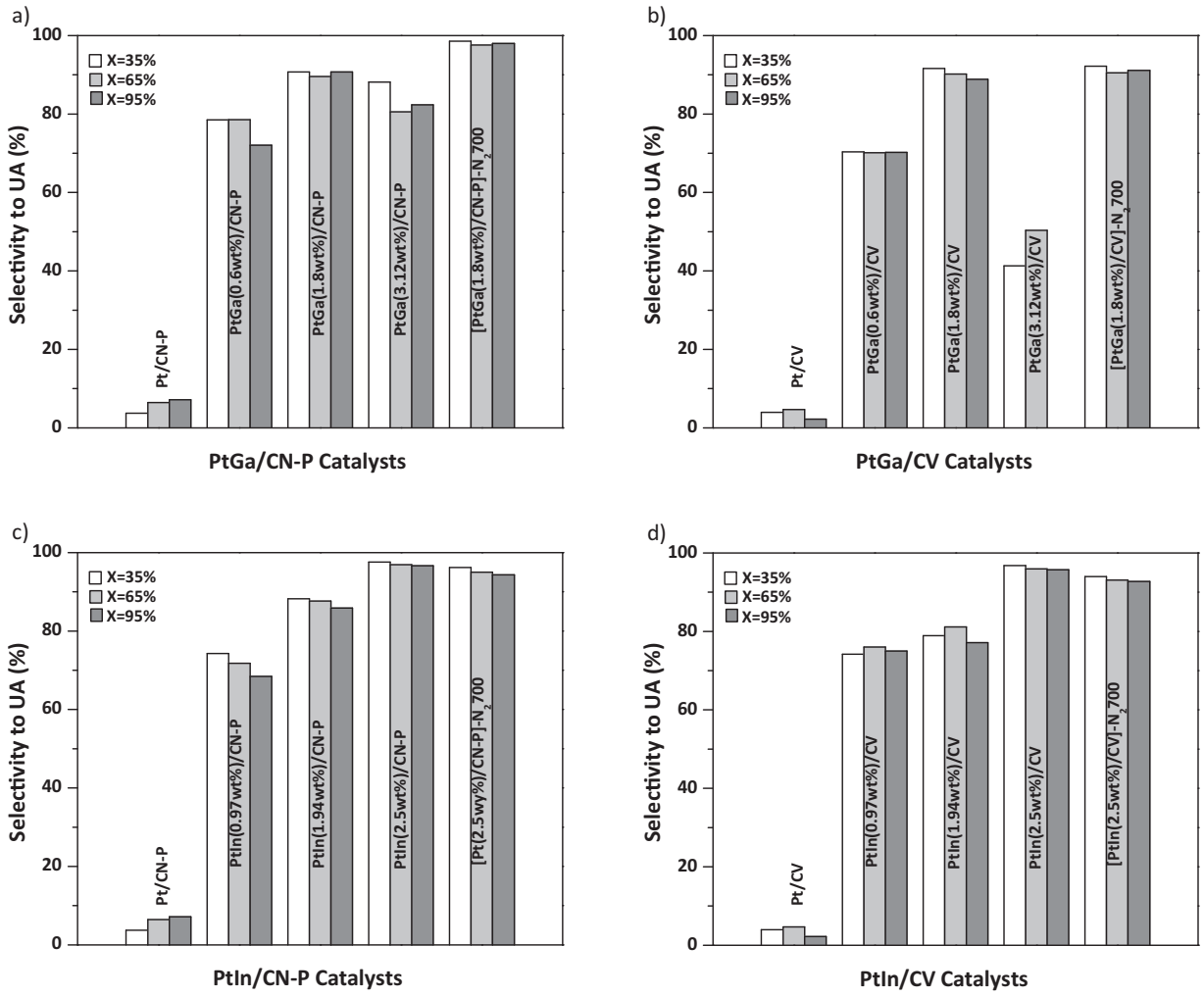


**Fig. 9.** Selectivities to UA measured at certain citral conversion levels (35, 65 and 95%) for the catalytic series: (a) PtGa/CN-P, (b) PtGa/CV, (c) PtIn/CN-P and (d) PtIn/CV.

postulated, considering that alloyed PtIn species could contribute to the increase of the selectivity to UA in the citral hydrogenation. According to several authors [16,17,52,53] and taking into account these results, it can be concluded that the alloy promotion mechanism would be based in the polarization of Pt–In species by shifting the electronic density from In to Pt as it was postulated for PtSn systems [9,54]. Positively charged In atoms would act as Lewis acid sites and favor the carbonyl group hydrogenation. The subsequent hydrogenation to citronellol would not take place over the alloy since UA would be vertically adsorbed hindering the activation of the C=C bond.

PtIn catalysts thermally treated with $N_2$ do not show an improvement in the selectivity to UA over both supports (Figs. 8 and 9). However, the activity of these catalysts is favored with the thermal treatment, reaching 95% citral conversion in a very short time compared with the untreated catalysts. This fact could be explained considering TEM results where the mean particle size slightly decreases with the $N_2$ thermal treatment, thus favoring the catalytic activity. However, this point would deserve a further research.

Even though slight differences in the catalytic results were found by using carbon nanotubes or carbon Vulcan as catalytic

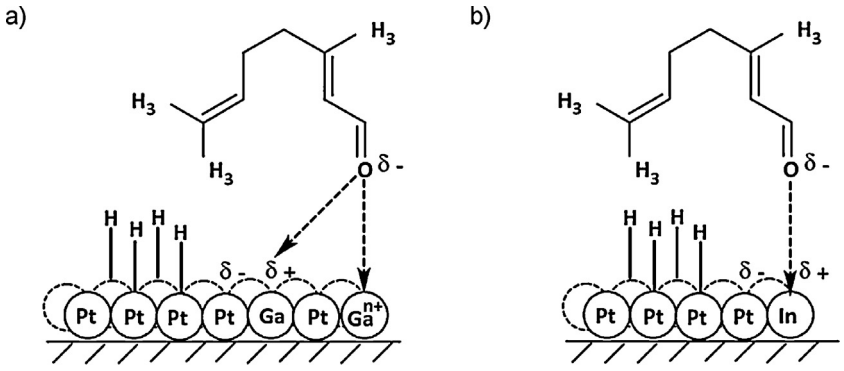


**Fig. 10.** Schemes of the proposed models for the promotion of C=O group in: (a) PtGa and (b) PtIn catalysts.

supports, it must be noted that some bimetallic catalysts used in this work show very good catalytic properties. Fig. 10 shows the mechanisms proposed for the studied bimetallic systems. These postulated mechanisms would help to understand the hydrogenation results. It must be noted that in PtGa catalysts two promoting effects take place, involving both alloyed and ionic species, while in PtIn catalysts the promoter effect is mainly given from alloyed species.

## 4. Conclusions

The second metal addition modifies the structure of Pt particles in a different way according to the nature of support (CN-P or CV) and promoter (Ga or In) producing an important increase in the selectivity to UA respect to the corresponding monometallic catalyst.

The surface of PtGa systems showed both ionic and zerovalent Ga species, the former ones producing mainly geometric (blocking/dilution) effects on the active phase and the latter ones would form Pt–Ga alloys that would disfavor the double C=C bond adsorption. It was necessary a Ga/Pt molar ratio equal to 1 to achieve an important modification of the metallic phase for both catalytic series. Both effects, geometric and electronic, explain the improvement in the performance of the bimetallic catalysts respect to monometallic ones. Ga ionic species act as Lewis acid sites polarizing the carbonyl group and easing its hydrogenation. The activity of the PtGa/CN-P series was higher than the PtGa/CV one and both of them were much higher than the corresponding monometallic catalysts. The $N_2$ thermal treatment reduced the activity for both series but the selectivities to UA were enhanced.

In PtIn catalysts, electronic effects were present and even with In/Pt molar ratios lower than 1, significant changes in the metallic phase were achieved. Pt–In particles show In (δ+) species, which could behave as Lewis acid sites and activate the carbonyl group. In these catalysts the promoter effect is mainly given from alloyed species. PtIn/CN-P series were more active than PtIn/CV one. Besides, the $N_2$ thermal treatment slightly reduced the selectivity to UA but increased the activity probably due to a rearrangement of the metallic phases. It is worth mentioning that the highest activity showed by [PtIn(2,5%)/CV]-$N_2$ catalysts could be related to the effect of the support over the catalytic activity.

## Acknowledgements

Authors thank to Miguel A. Torres, María Fernanda Mori and María Julia Yañez for the experimental assistance. This work was made with the financial support of Universidad Nacional del Litoral (Project CAI + D)-Argentina.

## References

[1] P. Mäki-Arvela, L.-P. Tiainen, R. Gil, T. Salmi, Stud. Surf. Sci. Catal. 108 (1997) 273–280.
[2] U.K. Singh, M.A. Vannice, Stud. Surf. Sci. Catal. 130 (2000) 497–502.
[3] F.V. Wells, M. Billot, Perfumery Technology, E. Horwood Publishers, Chichester, UK, 1981, pp. 149.
[4] T. Mallat, A. Baiker, Appl. Catal. A: Gen. 200 (2000) 3–22.
[5] E. Auer, A. Freund, J. Pietsch, T. Tacke, Appl. Catal. A: Gen. 173 (1998) 259–271.
[6] V. Ponec, Appl. Catal. A: Gen. 149 (1997) 27–48.
[7] M. Englisch, V.S. Ranade, J.A. Lercher, J. Mol. Catal. A: Chem. 121 (1997) 69–80.
[8] T.B.L.W. Marinelli, S. Nabuurs, V. Ponec, J. Catal. 151 (1995) 431–438.
[9] J.P. Stassi, P.D. Zgolicz, S.R. de Miguel, O.A. Scelza, J. Catal. 306 (2013) 11–29.
[10] E. Asedegbega-Nieto, A. Guerrero-Ruiz, I. Rodríguez-Ramos, Carbon 44 (2006) 804–806.
[11] Z.-T. Liu, C.-X. Wang, Z.-W. Liu, J. Lu, Appl. Catal. A: Gen. 344 (2008) 114–123.
[12] H. Ma, L. Wang, L. Chen, C. Dong, W. Yu, T. Huang, Y. Qian, Catal. Commun. 8 (2007) 452–456.
[13] F. Qin, W. Shen, C. Wang, H. Xu, Catal. Commun. 9 (2008) 2095–2098.
[14] E.L. Jablonski, A.A. Castro, O.A. Scelza, S.R. de Miguel, Appl. Catal. A: Gen. 183 (1999) 189–198.
[15] N. Nesterenko, O. Ponomoreva, V. Yuschenko, I. Ivanova, F. Testa, F. Di Renzo, F. Fajula, Appl. Catal. A: Gen. 254 (2003) 261–272.
[16] S.A. Bocanegra, O.A. Scelza, S.R. de Miguel, Appl. Catal. A: Gen. 468 (2013) 135–142.
[17] N. Homs, J. Llorca, M. Riera, J. Jolis, J.-L.G. Fierro, J. Sales, P.R. de la Piscina, J. Mol. Catal. A: Chem. 200 (2003) 251–259.
[18] E. Gebauer-Henke, J. Grams, E. Szubiakiewicz, J. Farbotko, R. Touroude, J. Rynkowski, J. Catal. 250 (2007) 195–208.
[19] N.S. Smirnova, D.A. Shlyapin, O.O. Mironenko, E.A. Anoshkina, V.L. Temerev, N.B. Shitova, D.I. Kochubey, P.G. Tsyrul'nikov, J. Mol. Catal. A: Chem. 358 (2012) 152–158.
[20] F. Domínguez, J. Sánchez, G. Arteaga, E. Choren, J. Mol. Catal. A: Chem. 228 (2005) 319–324.
[21] P.D. Zgolicz, J.P. Stassi, M.J. Yañez, O.A. Scelza, S.R. de Miguel, J. Catal. 290 (2012) 37–54.
[22] D.N. Blakely, G.A. Somorjai, J. Catal. 42 (1976) 181–196.
[23] C.R. Apesteguía, J. Barbier, Proceedings of the 8th Iberoam. Symp. on Catalysts, Huelva, Spain, 1982, p. 751.
[24] M. Boudart, Adv. Catal. 20 (1969) 153–166.
[25] J.E. Benson, M. Boudart, J. Catal. 4 (1965) 704–710.
[26] S.A. Bocanegra, S.R. de Miguel, I. Borbath, J.L. Margitfalvi, O.A. Scelza, J. Mol. Catal. A: Chem. 301 (2009) 52–60.
[27] C.D. Wagner, W.M. Riggs, L.E. Davis, J.F. Moulder, G.E. Muilenberg, Handbook of X-Ray Photoelectron Spectroscopy, Perkin-Elmer Co., Physical Electronics, 1979.
[28] S.R. de Miguel, J.I. Vilella, E.L. Jablonski, O.A. Scelza, C. Salinas-Martínez de Lecea, A. Linares-Solano, Appl. Catal. A: Gen. 232 (2002) 237–246.
[29] S.R. de Miguel, M.C. Román-Martínez, E.L. Jablonski, J.L.G. Fierro, D. Cazorla-Amorós, O.A. Scelza, J. Catal. 184 (1999) 514–525.
[30] S.R. de Miguel, O.A. Scelza, M.C. Román-Martínez, C. Salinas-Martínez de Lecea, D. Cazorla-Amarós, A. Linares Solano, Appl. Catal. A: Gen. 170 (1998) 93–103.
[31] M.C. Román-Martínez, D. Cazorla-Amorós, A. Linares-Solano, C. Salinas-Martínez de Lecea, Carbon 31 (1993) 895–902.
[32] F. Coloma, A. Sepúlveda-Escribano, J.L.G. Fierro, F. Rodríguez-Reinoso, Langmuir 10 (1994) 750–755.
[33] J.L. Figueiro, M.F.R. Pereira, M.M.A. Freitas, J.J.M. Órfão, Carbon 37 (1999) 1379–1389.
[34] A.B. da Silva, E. Jordão, M.J. Mendes, P. Fouilloux, Appl. Catal. A: Gen. 148 (1997) 253–264.
[35] B. Bachiller-Baeza, A. Guerrero-Ruiz, P. Wang, I. Rodríguez-Ramos, J. Catal. 204 (2001) 450–459.
[36] N. Mahata, F. Gonçalves, M.F.R. Pereira, J.L. Figueiredo, Appl. Catal. A: Gen. 339 (2008) 159–168.
[37] A.K. Shukla, M. Neergat, P. Bera, V. Jayaram, M.S. Hegde, J. Electroanal. Chem. 504 (2001) 111–119.
[38] N.H. Tran, M.A. Wilson, A.S. Milev, J.R. Bartlett, R.N. Lamb, D. Martin, G.S.K. Kannangara, Adv. Colloid Interface Sci. 145 (2009) 23–41.
[39] Y. Diaz, L. Melo, M. Mediavilla, A. Albornoz, J.L. Brito, J. Mol. Catal. A: Chem. 227 (2005) 7–15.
[40] C. Rameshan, W. Stadlmayr, S. Penner, H. Lorenz, L. Mayr, M. Hävecker, R. Blume, T. Rocha, D. Teschner, A. Knop-Gericke, R. Schlögl, D. Zemlyanov, N. Memmel, B. Klötzer, J. Catal. 290 (2012) 126–137.
[41] F. Rodríguez-Reinoso, Carbon 36 (1998) 159–175.
[42] M.C. Román-Martínez, D. Cazorla-Amorós, A. Linares-Solano, C. Salinas-Martínez de Lecea, Curr. Top. Catal 1 (1997) 17–46.
[43] S.A. Stevenson, J.A. Dumesic, R.T.K. Baker, E. Ruckenstein (Eds.), Metal–Support Interactions in Catalysis, Sintering and Redispersion, Van Nostrand Reinhold's Catalysis Series, New York, 1987.
[44] P.M. Ajayan, Chem. Rev. 99 (1999) 1787–1799.
[45] J.-M. Nhut, L. Pesant, J.-P. Tessonnier, G. Winé, J. Guille, C. Pham-Huu, M.-J. Ledoux, Appl. Catal. A: Gen. 254 (2003) 345–363.
[46] N. Homs, J. Llorca, P. Ramírez de la Piscina, F. Rodriguez-Reinoso, A. Sepúlveda-Escribano, J. Silvestre-Albero, Phys. Chem. Chem. Phys. 3 (2001) 1782–1788.
[47] I.M.J. Vilella, S.R. de Miguel, C. Salinas-Martínez de Lecea, A. Linares-Solano, O.A. Scelza, Appl. Catal. A: Gen. 281 (2005) 247–258.
[48] F. Coloma, J. Llorca, N. Homs, P. Ramírez de la Piscina, F. Rodríguez-Reinoso, A. Sepúlveda-Escribano, Phys. Chem. Chem. Phys. 2 (2000) 3063–3069.
[49] P. Mäki-Arvela, J. Hájek, T. Salmi, D.Yu. Murzin, Appl. Catal. A: Gen. 292 (2005) 1–49.
[50] C. Especel, D. Duprez, F. Epron, C. R. Chim. 17 (2014) 790–800.
[51] P. Sun, G. Siddiqi, W.C. Vining, M. Chi, A.T. Bell, J. Catal. 282 (2011) 165–174.
[52] P. Mériaudeau, A. Thangaraj, C. Naccache, Stud. Surf. Sci. Catal. 101 (1996) 1313–1320.
[53] J. Llorca, P. Ramírez de la Piscina, J. León, J. Sales, J.L.G. Fierro, N. Homs, Stud. Surf. Sci. Catal. 130 (2000) 2513–2518.
[54] F. Delbecq, P. Sautet, J. Catal. 220 (2003) 115–126.